NANO LETTERS

2004
Vol. 4, No. 5
853−857

Nanoscale Protein Patterning by Imprint Lithography

J. Damon Hoff,[†] Li-Jing Cheng,[‡] Edgar Meyhöfer,[§] L. Jay Guo,[‡,*] and Alan J. Hunt[†,*]

Department of Biomedical Engineering, Department of Electrical Engineering and Computer Science, and Department of Mechanical Engineering, University of Michigan, Ann Arbor, Michigan 48109

Received February 12, 2004; Revised Manuscript Received March 26, 2004

ABSTRACT

Selective localization of active proteins to patterns or specific sites is important for development of biosensors, bioMEMS, tissue engineering, and basic proteomic research. We present a flexible technique for selectively patterning bioactive proteins with nanoscale resolution using nanoimprint lithography and fluoropolymer surface passivation, and exploiting the specificity of the biotin/streptavidin linkage. This technique achieves high throughput reproducible nanoscale protein patterns with high selectivity and retained biofunctionality, as demonstrated by interactions between patterned antibodies and their antigen.

The biological roles of proteins are extraordinarily diverse and include catalysis, force generation, mechanical support, signaling, and sensing. Beyond their central importance to biology, proteins are of great interest because these subcellular nanomachines have potential to be integrated into micro- or nanofabricated devices to create low-cost, robust technologies of unprecedented small scale and high efficiency. Applications include biosensors, actuation of microelectromechanical systems (MEMS), and tissue engineering, as well as screening tools for proteomics and pharmacology, and basic biological research.[1−5] However, both the study and application of proteins have been challenged by the inherent difficulties associated with positioning these tiny objects. Thus, a primary enabling technology is the ability to precisely immobilize biomolecules in well-defined patterns while retaining their native functionality.

Toward achieving this goal, we have developed a technique for producing high-contrast and high-resolution protein patterns using nanoimprint lithography (NIL) and surface chemical modification. NIL offers the advantages of high throughput, low cost, high reproducibility, and the capability of creating nanopatterns with features as small as 10 nm over large areas.[6] In NIL, a Si template, fabricated by e-beam lithography or other suitable techniques, is pressed against a polymer-coated substrate heated to above the glass transition temperature of the polymer. After cooling, the template is removed from the substrate, leaving an imprint of the template features in the polymer. To immobilize proteins, the patterned substrate is then modified sequentially with an aminosilane, biotin, streptavidin, and finally our choice of biotinylated target protein. In this paper we show that our technique yields nanopatterned proteins that retain their biological functionality, as demonstrated by antigen binding by patterned antibodies. This technique is compatible with protein patterning on both oxidized Si wafers, which may take advantage of the wealth of microfabrication techniques developed by the semiconductor industry for integrating immobilized proteins into bioMEMS devices, and on optical quality coverglass suitable for microscopic analysis of protein distributions and interactions.

Many applications of patterned biomolecules can be enhanced by improving the resolution of the protein features. Smaller feature sizes enable, for example, the fabrication of high-density protein arrays for biosensors or proteomic screening, or facilitate studies of cellular interactions with small precisely located clusters of extracellular matrix proteins. A major advantage of the nanoimprint technique is that the feature size can be reduced to the nanoscale to create high-density arrays, or potentially control placement of individual proteins, while still retaining high throughput and reproducibility. Most previous work in protein patterning has relied ultimately on conventional photolithography to form a base template for protein adsorption, and has thus been constrained to micron-scale resolution by the light diffraction limit.[7] Dip-pen lithography[8−10] and e-beam patterning[11,12] are capable of nanoscale resolution, but these are relatively delicate serial processes and thus lack scalability. NIL provides an alternative method of patterning substrates

* Corresponding authors: guo@umich.edu and ajhunt@umich.edu.
† Department of Biomedical Engineering.
‡ Department of Electrical Engineering and Computer Science.
§ Department of Mechanical Engineering.

10.1021/nl049758x CCC: $27.50
Published on Web 04/13/2004

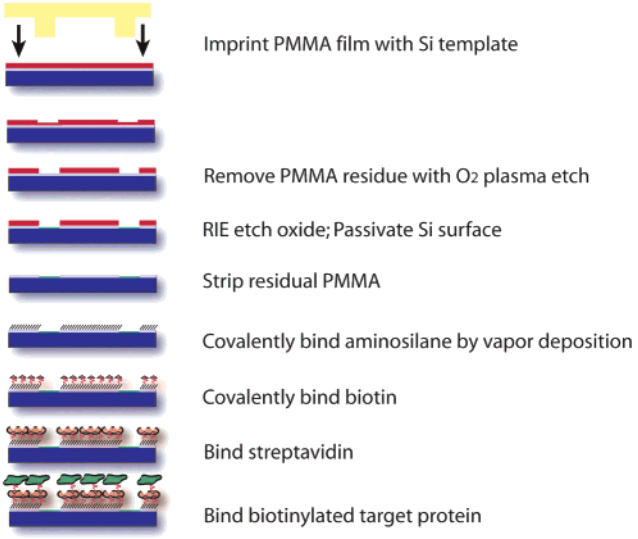

Figure 1. Process flow diagram of substrate patterning and protein immobilization. Spin-coated PMMA polymer is patterned by NIL. Exposed SiO_2 regions are etched and a passivating $(CF_x)_n$ polymer ($x = 1$ or 2, $n =$ number of monomer subunits, monomer MW = 31 or 50) is deposited during a CHF_3 RIE procedure. Residual PMMA is stripped away with acetone, exposing the underlying SiO_2 in the "patterned regions." An aminosilane monolayer is covalently attached to the exposed "patterned regions". Biotin-succinimidyl ester is then covalently linked to the primary amine of the aminosilane layer, and streptavidin is bound to the biotin layer. Finally, the biotinylated target protein is bound to the streptavidin layer.

with resolutions down to sub-10 nm, on the scale of individual protein molecules.

The most important criterion for any protein patterning technique is specific binding of target proteins, i.e., the technique must produce a high density of biomolecules in desired regions ("patterned regions") while preventing adsorption of these molecules in other regions ("unpatterned regions"). To satisfy this criterion we selectively passivate a substrate with a base pattern of an inert, nonpolar $(CF_x)_n$ ($x = 1$ or 2, $n =$ number of monomer subunits, monomer MW = 31 or 50) polymer[13,14] coating to establish a template for the selective attachment of target linker molecules for highly specific covalent binding of biotin, which serves as a target for generalized protein binding through strong noncovalent biotin−streptavidin interactions.

Figure 1 schematically illustrates the patterning process. A silicon mold was fabricated by standard e-beam lithography and dry etching. To facilitate mold separation after imprinting, the mold was coated with surfactant, perfluorochlorosilane (Lancaster Synthesis, Windham, NH) to provide a low energy surface. The material to be imprinted, poly(methyl methacrylate) or PMMA (Aldrich, St. Louis, MO) was spun onto a substrate of either 60 nm thick silicon oxide thermally grown on silicon or onto optical grade glass wafers (Erie Scientific, Portsmouth, NH). The PMMA was patterned by NIL: the mold and substrate were brought into physical contact at 175 °C, and a pressure of 50 kg/cm^2 was applied for 5 min before cooling to room temperature. After the mold and substrate were separated, O_2 reactive ion etching (RIE) was used to remove PMMA residual in the patterned regions (O_2 gas flow = 20 sccm, pressure = 20 mTorr, power = 50 W) and CHF_3 RIE was used to etch the newly exposed oxide (CHF_3 gas flow = 40 sccm, O_2 gas flow = 5 sccm, pressure = 20 mTorr, power = 150 W), transferring the patterns to the oxide layer. In addition to etching away the exposed SiO_2 to the underlying Si substrate, this etching process deposits a thin passivating layer of CF_x polymer residue on the newly exposed Si surface.[13,14] The presence of this passivating polymer residue was verified by X-ray energy dispersive spectroscopy (XEDS). The remaining PMMA was then removed by sonication in acetone, leaving exposed SiO_2 regions separated by regions of CF_x-passivated Si. Note that it is not necessary to etch down to the Si surface, as evidenced by the success of using the same fabrication procedure on glass substrate.

The exposed oxide pattern selectively reacts with an aminosilane to form a covalently bound monolayer. We found aminopropyldimethylethoxysilane (APDMES, SIA0603.0, Gelest, Morrisville, PA) to be particularly effective. The single alkoxy group on the head of this silane ensures the reproducible deposition of a well-formed monolayer by minimizing unwanted self-polymerization.[15−18] Producing good silane monolayers on exposed silicon oxide or glass requires careful attention to procedure, especially with regards to temperature and humidity. NIL-patterned substrates were heated to 70 °C under dry nitrogen in a 0.4 L glass chamber. A 5 μL portion of APDMES was injected into the chamber through an airtight septum and allowed to react for 20 min with the exposed SiO_2 surfaces before venting with fresh nitrogen for 90 s. Samples were then sonicated for 10 min in dry isooctane, followed by ethanol, then 1 mM NaOH to remove unbound silane from the surface and deprotonate the exposed amine. Deprotonation of the amine ensures the monolayer's reactivity to subsequent modifications by nucleophilic substitution reactions. The specificity of the aminosilane deposition was initially quantitatively verified by covalently binding tetramethylrhodamine succinimidyl ester (C-1171, Molecular Probes, Eugene, OR) to the amine tail group of the aminosilane monolayer via an *n*-hydroxysuccinimide reaction and measuring the resulting fluorescent intensities in the aminosilane patterned regions and the passivated Si regions. A very bright signal was observed in the aminosilane patterned regions, corresponding to a surface density of aminosilane on the order of a monolayer; no detectable fluorescent signal was detected on the passivated regions, indicating the aminosilane does not react with the passivated Si surface. Therefore the plasma deposition of the fluoropolymer layer is responsible for the high differentiation between the two regions.

At this point, the APDMES-functionalized substrate is enclosed in a flow cell, 2.2 cm long by approximately 50 μm deep and 0.5 cm wide, formed by fixing a glass cover slip to the top of 50 μm thick aluminum foil spacers adhered to the substrate with vacuum grease. This allows sequential introduction of various buffers to the substrate, and also allows easy imaging using epifluorescence microscopy. Biotin is covalently bound to the exposed primary amine tail group of the patterned APDMES by filling the flowcell

with a 68 μM biotin−succinimidyl ester solution (B-1513, Molecular Probes, Eugene, OR) in 0.1 M HEPES buffer at pH 7.65 for 20 min before flushing the flowcell with either deionized water or a biological buffer such as BRB80 (80 mM PIPES, 1 mM $MgCl_2$, 1 mM EGTA, brought to pH 6.8 with KOH). Next a streptavidin layer is deposited and bound to the biotin layer by flushing the flowcell with a 10 μg/mL streptavidin solution in blocking buffer (0.1 M HEPES, pH 7, containing 5 mg/mL BSA) and incubating for 15 min. The resultant streptavidin monolayer serves as a base for the specific adsorption of any biotinylated target protein.

Biotinylated BSA served as our initial target protein. The target protein was bound by flushing the flowcell with a 50 μg/mL biotinylated BSA solution in blocking buffer and incubating for 10 min. For fluorescent imaging, the heavily biotinylated BSA was further exposed to a 10 μg/mL rhodamine-labeled streptavidin (S-870, Molecular Probes, Eugene, OR) solution in Blocking Buffer for 10 min. The flowcell was rinsed with 0.1 M HEPES, pH 7 containing an oxygen scavenging antifade cocktail (30 mM glucose, 0.6 mg/mL glucose oxidase, 0.12 mg/mL catalase in BRB80) prior to transfer to the microscope stage.

To quantify the surface density of target protein in the patterned regions we calibrated the measured fluorescent intensity of immobilized fluorescently labeled proteins to solutions of the same proteins at known concentration. Fluorescent images of patterned target proteins were captured on a Zeiss Axioplan 2 microscope fitted with a CoolSNAPcf CCD camera (Roper Scientific, Trenton, NJ). The fluorescent intensity per molecule in the plane of focus was derived briefly as follows.

The total fluorescent intensity captured by the camera, I_C, imaging a flowcell of known depth is

$$I_C = k_{CCD} I_E = k_{CCD} \int_z \int_r q N_F I_I(z) A(z) \phi(z,r)\, dr\, dz$$

where k_{CCD} is a constant relating the intensity of light incident on the camera's CCD chip to the camera's electrical signal, I_E is the total fluorescent emission captured, q is the quantum efficiency of the fluorophore, N_F is the concentration of fluorophore in solution, I_I is the intensity of the illuminating (excitation) light as a function of chamber depth z, A is the area of the illuminated field of view at depth z, and φ is the percentage of emitted light from each fluorophore that is captured by the objective lens at depth z and lateral distance r from the center of the image plane.

The illumination $I_I(z)$ can be expressed as

$$I_I(z) = I_0 \frac{r_0^2}{(r_0 + z\tan\theta)^2}$$

where I_0 is the illumination in the plane of focus, r_0 is the illumination spot size in the plane of focus, and θ is half the angular aperture ($NA = n\sin\theta$).

In practice, a flowcell is formed by fixing a glass cover slip to the top of 50 μm thick aluminum foil spacers adhered to the substrate with vacuum grease. A solution of blocking buffer (0.1 M HEPES, pH 7, containing 5 mg/mL BSA) is added to the flowcell to saturate the flowcell surfaces to prevent fluorophore from binding nonspecifically. After about one minute, the flowcell is flushed with three flowcell volumes of a solution containing 5 mg/mL BSA and a known concentration of the same fluorophore that was patterned on the sample of interest. The particular concentration of fluorophore varies by sample and is chosen such that when imaged under conditions (illumination intensity, exposure time, etc.) identical to those used when imaging the patterned sample of interest, the measured intensity lies within the dynamic range of the camera. Images of this calibration flowcell are then taken near the upper surface of the chamber immediately after imaging the patterned substrate, as the lamp intensity slowly drifts over time. To subtract the background autofluorescence and camera dark current, another flowcell is fabricated and filled with blocking buffer. This flowcell is imaged similarly to the fluorescent calibration flowcell above. The intensity from this background sample is then subtracted from the intensity measured from the fluorescent calibration flowcell to get the experimental value for I_C. Because the imaging conditions and fluorophore used on the sample of interest and fluorescent calibration flowcell are identical, many of the terms in the equation for I_C above can be lumped together, greatly simplifying the computation (e.g., k_{CCD}, q, I_0, and θ are the same in all samples). Considering potential errors stemming from geometric estimations (i.e., depth of the flowcell), light source instability, electrical noise, and reflectance of fluorophore emittance off of the SiO_2 substrate, we estimate the maximum error in this measurement to be approximately 30%.

This analysis shows a surface density of rhodamine-labeled streptavidin in the patterned region of approximately 120 000 molecules/μm^2, which is on the same order as the surface density expected from a close-packed streptavidin monolayer. Applying this analysis to the passivated Si region, we find the coverage of target protein in this region is undetectable, giving an upper limit of approximately 50 molecules/μm^2, or less than 0.1% of a monolayer. This demonstrates nearly complete monolayer coverage of target biomolecule in the patterned regions, with only a negligible amount of target protein adsorbed to the passivated regions.

One of the main advantages of using NIL technology in patterning is the ability to push the resolution to nanometer scales. To verify our ability to generate nanoscale protein patterns, we fabricated a mold to create 75 nm wide lines on Si substrates (Figure 3). These nanopatterned substrates were prepared identically to the microscale substrates, with biotinylated BSA as the target protein and rhodamine-labeled streptavidin subsequently bound for fluorescent imaging. The surface density measured by fluorescence is consistent with that observed on the micropatterned substrates, indicating an approximate monolayer of adsorbed target protein on the nanolines.

Broadly useful patterning technology requires that immobilized proteins retain their biological functionality. We have demonstrated that the functionality of patterned anti-

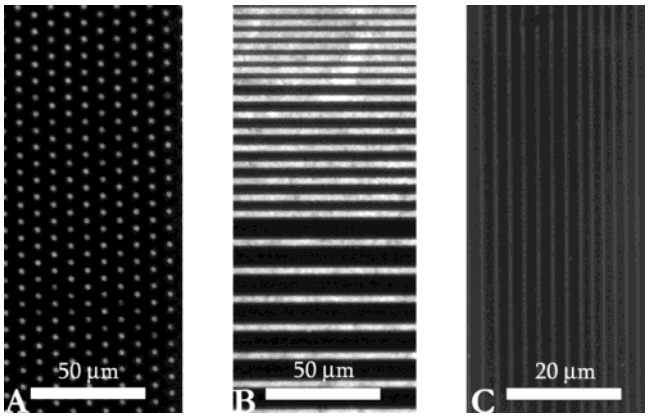

Figure 2. Epi-fluorescence image of rhodamine-labeled streptavidin bound to sharp uniform microscale dots (A) and lines (B) of biotinylated BSA protein on oxidized Si substrates. Fluorescent intensity signal in the passivated regions is at or below the noise level of the imaging system, indicating the fluorophore concentration in these areas is less than 0.1% of that observed in the patterned regions. (C) Rhodamine-labeled streptavidin bound to patterns of immobilized biotinylated BSA on cover glass.

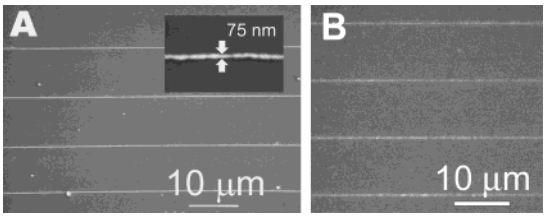

Figure 3. Proteins patterned onto sub-100 nm features. (A) SEM image of oxide nanolines formed on a Si substrate by NIL and RIE. (Inset) Close-up SEM of oxide nanoline, showing a line width of less than 100 nm. (B) Fluorescence micrograph of nanolines after patterning with biotinylated BSA and binding rhodamine-labeled streptavidin. Analysis of the fluorescent intensity along the line indicates an approximate monolayer of target protein.

bodies is retained by patterning the target protein goat anticatalase (ab6572, Novus Biologicals, Littleton, CO) and observing its binding of fluorescently labeled catalase from solution. Substrates were prepared as described above up to the streptavidin layer. A 10 μg/mL solution of biotinylated anticatalase in blocking buffer was then introduced into the flowcell for 10 min. The flowcell was flushed with HEPES pH 7.0, and a 50 μg/mL solution of rhodamine-labeled catalase in blocking buffer was introduced. This solution was incubated 10 min before rinsing with 0.1 M HEPES pH 7.0 containing antifade. Fluorescent images show that the labeled catalase binds to the immobilized anticatalase in the patterned regions (Figure 4), while only a negligible amount binds in unpatterned regions. Quantifying the fluorescent intensity of the bound catalase as explained above yields a surface density of approximately 31 000 catalase molecules/μm^2, again on the order of a monolayer. One can easily imagine extending this technique to create ultrahigh density antibody arrays for applications such as compact sensors and diagnostic devices, and for proteomic screening. The ability to specifically place small numbers of protein molecules at desired locations will also benefit biophysical and molecular biology studies, as

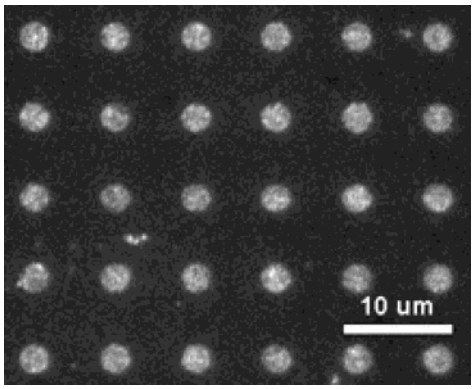

Figure 4. Epi-fluorescence image demonstrating the retained biological activity of patterned biomolecules. Biotinylated polyclonal anticatalase antibody was patterned in 2 μm dots, and the antibody's fluorescent antigen, rhodamine-labeled catalase, selectively binds to the antibody-patterned regions. The surface density of the bound catalase is approximately 31 000 molecules/μm^2.

well as integration of protein activities into microscale devices (e.g., bioMEMS).

In summary, we have developed a technique for immobilizing biomolecules with nanoscale resolution in a process that preserves functionality of the immobilized proteins. The use of nanoimprinting as the patterning method for the initial template enables high throughput ultrahigh resolution patterning. Because our method relies on well-established and high affinity biotin−streptavidin binding, it can be applied to pattern virtually any protein, without the high degree of variability expected when protein is immobilized by virtue of more general chemical properties (i.e., hydrophobicity or charge). The target proteins bind specifically to the ligand patterns, and the nonspecific adsorption is at least 1000-fold lower in the region of the passivation layer. We have demonstrated feature sizes down to 75 nm, and since nanoimprinting allows for features as small as 10 nm across,[6] we anticipate that placement of individual biomolecules will be possible. The compatibility of this technique with both SiO_2 substrates as well as optical quality cover glass broadens the potential applications of immobilized proteins, allowing easy integration with MEMS technologies as well as ready access to a wide range of optical imaging, measurement, and manipulation methods.

This versatile, highly specific, and biologically friendly technique for generating ultrahigh-resolution protein patterns will allow the diverse activities of proteins to be integrated into microfabricated devices and sensors. For example, protein chips, arrayed with a myriad of proteins, are becoming a useful tool in proteomics, enabling quick parallel screening of potential protein−protein interactions in large protein populations; as well as in more focused diagnostic biosensors, concentrated on analysis of enzymatic interactions within a smaller set of proteins. When expanded to allow patterning of multiple proteins on a single substrate, the high contrast and resolution this technique provides will allow fabrication of chips with protein feature densities more than an order of magnitude greater than those currently available, potentially improving sensitivity, reducing required analyte

volumes, and increasing the number of proteins that can be screened against on a single chip.

Acknowledgment. The authors thank Stefan Lakämper, Joseph Bull, and Chih-Ting Lin for helpful discussions. The authors thank Chung-Yen Chao for his assistance in electron-beam lithography. This work was supported in part by DARPA, NSF, and the Burroughs-Wellcome Fund.

References

(1) Kane, R. S.; Takayama, S.; Ostuni, E.; Ingber, D. E.; Whitesides, G. M. *Biomaterials* **1999**, *20*, 2363−2376.
(2) Singhvi, R.; Kumar, A.; Lopez, G. P.; Stephanopoulos, G. N.; Wang, D. I. C.; Whitesides, G. M.; Ingber, D. E. *Science* **1994**, *264*, 696−698.
(3) MacBeath, G.; Schreiber, S. L. *Science* **2000**, *289*, 1760−1763.
(4) Douvas, A.; Argitis, P.; Misiakos, K.; Dimotikali, D.; Petrou, P. S.; Kakabakos, S. E. *Biosens. Bioelectron.* **2002**, *17*, 269−278.
(5) Stjohn, P. M.; Kam, L.; Turner, S. W.; Craighead, H. G.; Issacson, M.; Turner, J. N.; Shain, W. *J. Neurosci. Methods* **1997**, *75*, 171−177.
(6) Chou, S. Y.; Krauss, P. R.; Zhang, W.; Guo, L. J.; Zhuang, L. *J. Vacuum Sci. Technol. B* **1997**, *15*, 2897−2904.
(7) Blawas, A. S.; Reichert, W. M. *Biomaterials* **1998**, *19*, 595−609.
(8) Liu, G. Y.; Amro, N. A. *Proc. Natl. Acad. Sci. U.S.A.* **2002**, *99*, 5165−5170.
(9) Lee, K. B.; Park, S. J.; Mirkin, C. A.; Smith, J. C.; Mrksich, M. *Science 295*, 1702−1705.
(10) Wilson, D. L.; Martin, R.; Hong, S.; Cronin-Golomb, M.; Mirkin, C. A.; Kaplan, D. L. *Proc. Natl. Acad. Sci. U.S.A.* **2001**, *98*, 13660−13664.
(11) Glezos, N.; Misiakos, K.; Kakabakos, S.; Petrou, P.; Terzoudi, G. *Biosens. Bioelectron.* **2002**, *17*, 279−282.
(12) Harnett, C. K.; Satyalakshmi, K. M.; Craighead, H. G. *Appl. Phys. Lett.* **2000**, *76*, 2466−2468.
(13) Coburn, J. W.; Winters, H. F. *J. Vac. Sci. Technol.* **1979**, *16*, 391−403.
(14) Oehrlein, G. S.; Matsuo, P. J.; Doemling, M. F.; Rueger, N. R.; Kastenmeier, B. E. E.; Schaepkens, M.; Standaert, T.; Beulens, J. J. *Plasma Sources Sci. Technol.* **1996**, *5*, 193−199.
(15) Kallury, K. M. R.; Macdonald, P. M.; Thompson, M. *Langmuir* **1994**, *10*, 492−499.
(16) Moon, J. H.; Shin, J. W.; Kim, S. Y.; Park, J. W. *Langmuir* **1996**, *12*, 4621−4624.
(17) Pallandre, A.; Glinel, K.; Jonas, A. M.; Nysten, B. *Nano Lett.* **2004**, *4*, 365−371.
(18) White, L. D.; Tripp, C. P. *J. Colloid Interface Sci.* **2000**, *232*, 400−407.

NL049758X